ARTICLE

Soft, Highly Conductive Nanotube Sponges and Composites with Controlled Compressibility

Xuchun Gui,[†] Anyuan Cao,[‡,*] Jinquan Wei,[†] Hongbian Li,[‡] Yi Jia,[†] Zhen Li,[†] Lili Fan,[†] Kunlin Wang,[†] Hongwei Zhu,[†] and Dehai Wu[†,*]

[†]Key Laboratory for Advanced Materials Processing Technology, Ministry of Education, Department of Mechanical Engineering, Tsinghua University, Beijing 100084, P. R. China, and [‡]Department of Advanced Materials and Nanotechnology, College of Engineering, Peking University, Beijing 100871, P. R. China

ABSTRACT Porous carbon nanotube networks represent a type of material that can achieve both structural robustness and high flexibility. We demonstrate here controlled synthesis of soft to hard sponges with densities ranging from 5 to 25 mg/cm^3, while retaining a porosity of >99%. The stable sponge-like structure allows excellent compressibility tunable up to 90% volume shrinkage, and the ability to recover most of volume by free expansion. Electrical resistivity of the sponges changes linearly and reversibly after 300 cycles of large-strain compression. Nanotubes forming the three-dimensional scaffold maintain good contact and percolation during large-strain deformation, polymer infiltration, and cross-linking process, suggesting potential applications as strain sensors and conductive nanocomposites.

KEYWORDS: CNT sponges · nanotubes · conductive nanocomposites · electrical resistivity · compressibility

Natural and synthetic sponge-like products have potential applications as tissue scaffolds, biological sensors, mechanical actuators, catalytic supports, and oil spill remediation.[1−10] Many of these applications require that the material have high porosity, flexibility, and robustness under mechanical strains.[2,3,10] For applications such as sensors, actuators, and electrodes, it is important to make porous materials with high electrical conductivity.[2−7] It has been challenging to synthesize structures possessing a combination of high porosity, flexibility, and conductivity. Silica-based and other nanostructure-based aerogels are typically very fragile, especially under compression.[11,12] Recently, there has been growing interest in developing sponge-like materials by coating carbon nanotubes (CNTs) onto a collagen scaffold or yarning CNT−DNA hybrid fibers.[1,2] Owing to the mechanical strength of CNTs and strong interaction with protein molecules, the sponge fibers are flexible and tough.[2] Because of their chemical stability and biocompatibility, CNTs coated on a collagen surface can enhance cell adhesion and growth.[1]

Porous structures such as CNT forests, aerogels, foams, and CNT-carbon particle hybrids can be used as supercapacitor electrodes, nanocomposites, photosensors, and chemical sensors.[13−18] For example, aligned CNT arrays have been infiltrated with polymers to make composites for thermal management, field emission, and conductive probes.[16−18] So far, control of the microstructure, porosity, and mechanical properties by manipulating CNT interaction and morphology remains a difficult task. Many CNT-based structures do not show appreciable compressibility and springiness, and tend to collapse or flatten under compression. Although the CNT aerogel can be reinforced by polymer infiltration, the resulting composite showed significantly decreased electrical conductivity (by 5 orders of magnitude).[19] Recently, we reported a CNT sponge in which nanotubes are interconnected into a three-dimensional framework and its environmental application such as oil absorption.[10] Here, we show controlled synthesis of CNT sponges in relatively soft to hard forms with tailored compressibility over a wide strain range (up to 90%). Soft and compressible sponges are particularly useful as compliant bioimplants or structural media. As CNTs form a conductive and stable network, a compressible strain sensor is demonstrated here. The porous structure also allows direct polymer infiltration without disturbing the CNT interconnection, resulting in a sponge composite with high electrical conductivity.

The CNT sponges are produced in a chemical vapor deposition (CVD) system where a mixture of carbon source (dichlorobenzene) and catalyst precursor (fer-

*Address correspondence to anyuan@pku.edu.cn, wdh-dme@tsinghua.edu.cn.

Received for review January 20, 2010 and accepted March 23, 2010.

Published online April 1, 2010. 10.1021/nn100114d

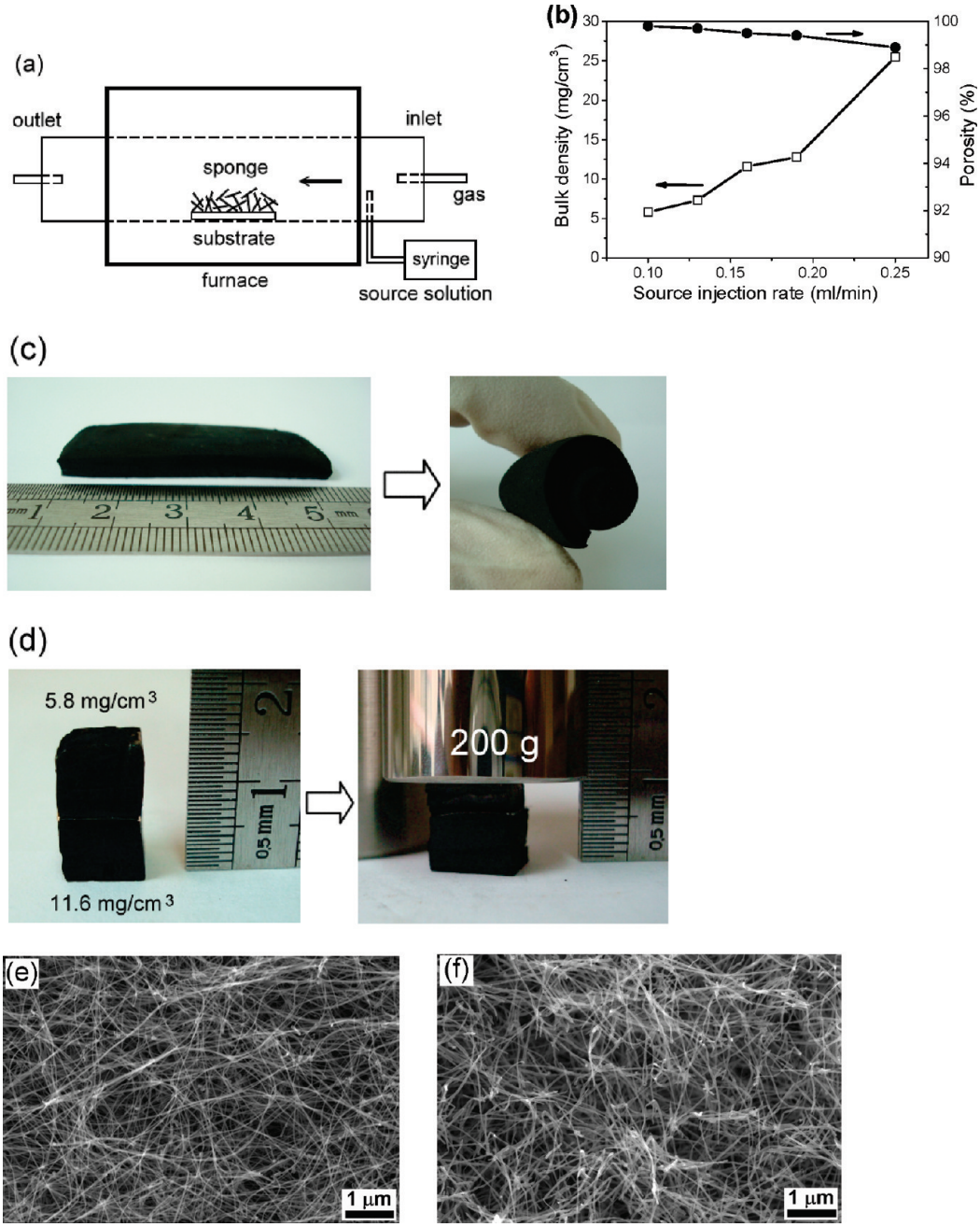

Figure 1. Soft sponges with controlled density and porosity. (a) Illustration of the CVD method for producing sponges. The source solution containing ferrocene and dichlorobenzene was constantly injected into the furnace by a syringe pump. Carbon nanotubes grow on the quartz substrate and overlap into the porous sponge structure. (b) Measured bulk density and porosity of sponges depending on the source injection rate. The porosity remains high (>99%) while the density increases by 5 folds. (c) Pictures of a soft carpetlike sponge which can be rolled up tightly. (d) Pictures of two stacked sponges supporting a weight of 200 g, in which the top sponge was compressed to a larger degree due to its lower density (5.8 mg/cm^3). (e) SEM images showing a random CNT network of a sponge with a density of 5.8 mg/cm^3. (f) CNT network of the sponge with a higher density of 25.5 mg/cm^3.

rocene) was injected into the furnace at a constant rate by a syringe pump (Figure 1a). During growth, CNTs stack as multilayers in a random manner to form mm-thick sponges. Variation of the source injection rate from 0.10−0.25 mL/min resulted in sponges with bulk densities of about 5.8 to 25.5 mg/cm^3 (Figure 1b). The average outer diameter of CNTs increases from 32 to 44 nm, while the inner diameter remains about 16 nm. The increase of sponge density is due to the formation of more numbers of CNTs per unit volume at higher source injection rate, as well as the formation of larger-diameter CNTs. While we see a 5-fold increase of density, the sponges maintain a high porosity with slight dropping from 99.8% to 98.9% (Figure 1b). The random (*versus* aligned) stacking of CNTs ensures continuous expanding of the porous structure rather than filling of pore volume at higher densities.

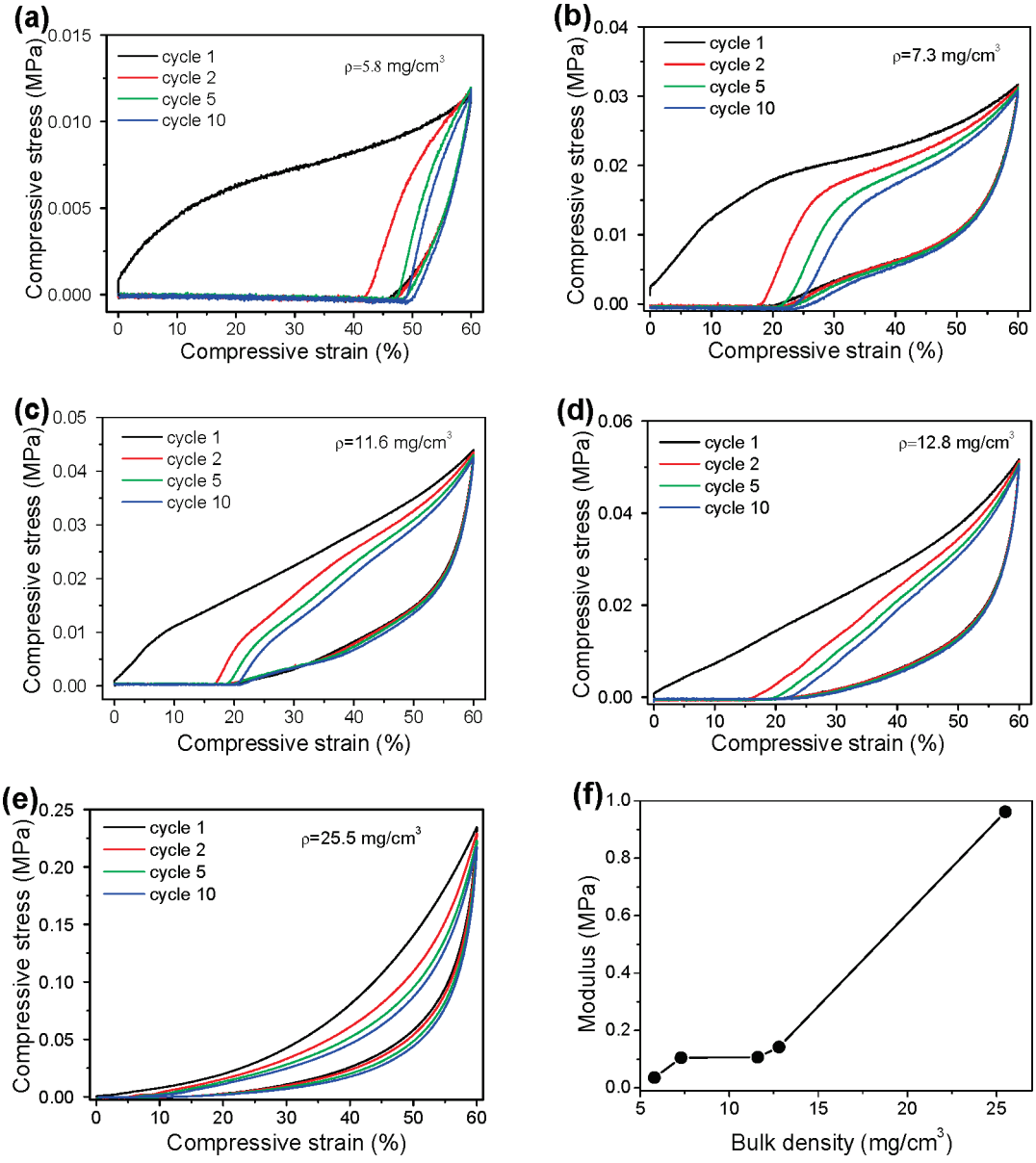

Figure 2. Mechanical properties of CNT sponges. Stress−strain curves of sponges with densities of (a) 5.8 mg/cm^3, (b) 7.3 mg/cm^3, (c) 11.6 mg/cm^3, (d) 12.8 mg/cm^3, and (e) 25.5 mg/cm^3. Each sample was compressed to a maximum strain of ε = 60% for 10 cycles. (f) Calculated stiffness (Young's modulus) of the above sponges. The modulus was calculated based on the highest slope of the stress curve in the first cycle of each sample.

The as-grown lowest-density (5.8 mg/cm^3) sponge appears as a black carpet with an area of about 12 cm^2 and a thickness of 3.5 mm. This soft and flexible sponge can be manipulated into tight scrolls without splitting of structure (Figure 1c). Sponges with lower densities can be compressed more easily than larger density samples. When two sponge bricks with density of 5.8 and 11.6 mg/cm^3, respectively, are placed in series to support a standard weight of 200 g, the smaller density brick shows much larger deformation under the same compressive force (Figure 1d). They also show different degrees of volume recovery after removing the weight. Scanning electron microscopy (SEM) examination of the inside area reveals that both low and high density sponges have a porous structure made of randomly interconnected CNTs (Figure 1e,f).

We have done systematic mechanical testing on sponges with various densities to study their compressive strength, compressibility, and recoverability. Cyclic stress−strain curves show that all sponges can be compressed to large strains (ε = 60%) at relatively lower stress levels (0.01 to 0.25 MPa) (Figure 2a−e). The compressive strength has consistently increased by 20 fold increases when the sponge density changed from 5.8 to 25.5 mg/cm^3. The sponge recovery takes about 3 min when the compression stage is set to retreat at a speed of 2 mm/min, and could be as fast as a few seconds at a much higher testing speed (80 mm/min). For low-density and relatively soft sponges (5.8 and 7.3 mg/

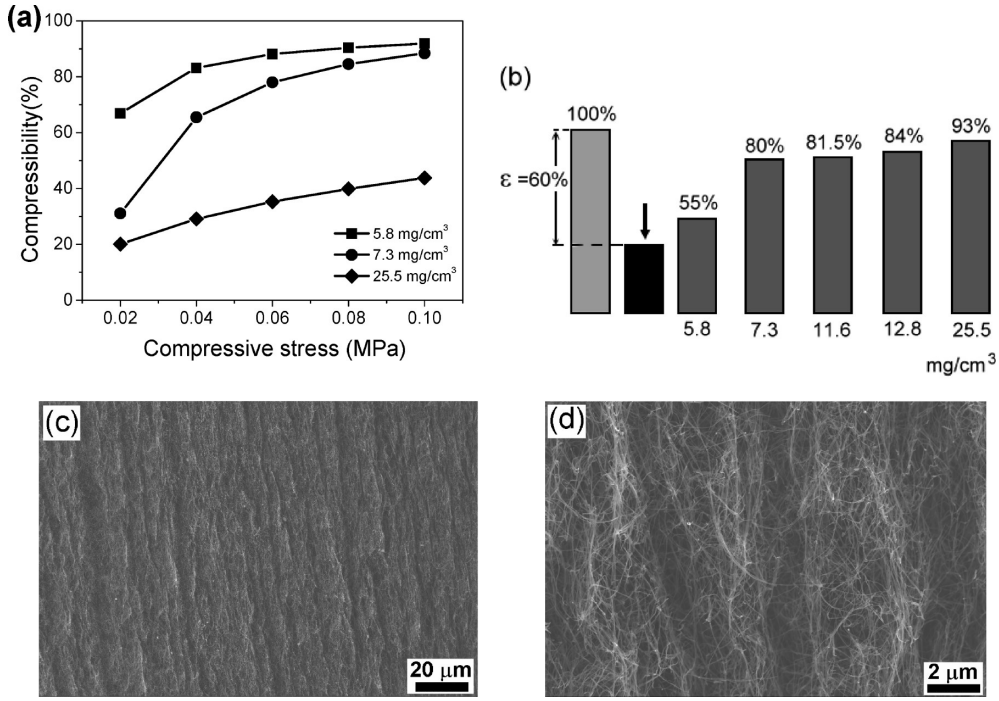

Figure 3. Compressibility and recoverability of CNT sponges. (a) Compressibility of sponges with different densities at applied stress. Without lateral expansion during compression, the compressibility (volume reduction) equals to compressive strain. (b) Thickness recovery of sponges with five densities (illustrated in a column shape) upon unloading from a compressed state ($\varepsilon = 60\%$). (c) SEM image of the rippled structure in the sponge formed under compression. (d) Enlarged view showing reorientation of some CNTs along the direction perpendicular to the compressive stress.

cm^3), a wide-range stress plateau can be clearly revealed in the first-cycle loading, which has gradually diminished for higher-density sponges. While soft sponges (5.8 mg/cm^3) show very large plastic deformation (close to 50%) in the first cycle, such deformation has dropped to less than 10% in relatively hard sponges, indicating enhanced structural recovery with increasing sponge density. Despite that, all of these sponges have very small stiffness (Young's modulus $<$ 0.1 MPa) (Figure 2f) that is 3 to 4 orders of magnitude lower than previously reported aligned CNT arrays and composites ($\sim$100 MPa to 1 GPa).[18,20,21] When tested in different directions, the compressive behavior is isotropic.[10]

The sponges show tunable compressibility over a wide range depending on the material density and compressive stress (Figure 3a). At a density of 5.8 mg/cm^3, the sponge can be compressed to a densified form with 90% volume reduction under a stress of 0.1 MPa. In comparison, high density (25.5 mg/cm^3) sponge exhibits only 40% volume shrinkage under the same stress level. These results indicate that it is possible to control the sponge porosity and manipulate the sponge shape by means of mechanical compression or densification. The soft sponges also show certain degrees of shape and structural recovery after load removal. They could spring back to 80% to 93% of original thickness from a heavily compressed condition ($\varepsilon =$ 60%) (Figure 3b). The ability to expand and recover a porous structure is unique compared with many brittle aerogels. Under uniaxial compression, the CNT framework exhibit ripple-like morphology with a periodicity of 2$-$5 μm, and these ripples can be further folded to accommodate large-strain deformation (Figure 3c). Formation of ripple bands across the sponge structure is due to the coordinated reorientation of CNTs in the direction perpendicular to compressive stress (Figure 3d). However, the rippling of random CNTs in the sponge is not as regular as the buckling of aligned CNTs as reported previously.[20,22]

Finally, we demonstrate that these springy sponges can be used to construct strain sensors as well as conductive composites by direct polymer infiltration. The two-probe electrical resistivity was monitored *in situ* during the compression process by attaching thin silver wires to the top and bottom sponge surface between the compression stages (Figure 4a). The sponge resistivity showed a reversible change in the cycle, decreasing by about 20% (from 2.1 down to 1.7 $\Omega \cdot$ cm) during compression to $\varepsilon = 60\%$ and returning to almost original value upon unloading (Figure 4b). Proportional sponge densification under constant-rate compression could cause resistivity decrease. Similar resistivity change was also observed in an aligned CNT forest under compression (from about 0.27 down to 0.21 $\Omega \cdot$ cm).[23] The behavior is consistent over five cycles without degradation of sponge conductivity, indicating that the CNT framework is very stable (Figure 4c). Fatigue tests show that the sponge maintains a resistivity linearly changing between 2.2 and 2.4 $\Omega \cdot$ cm af-

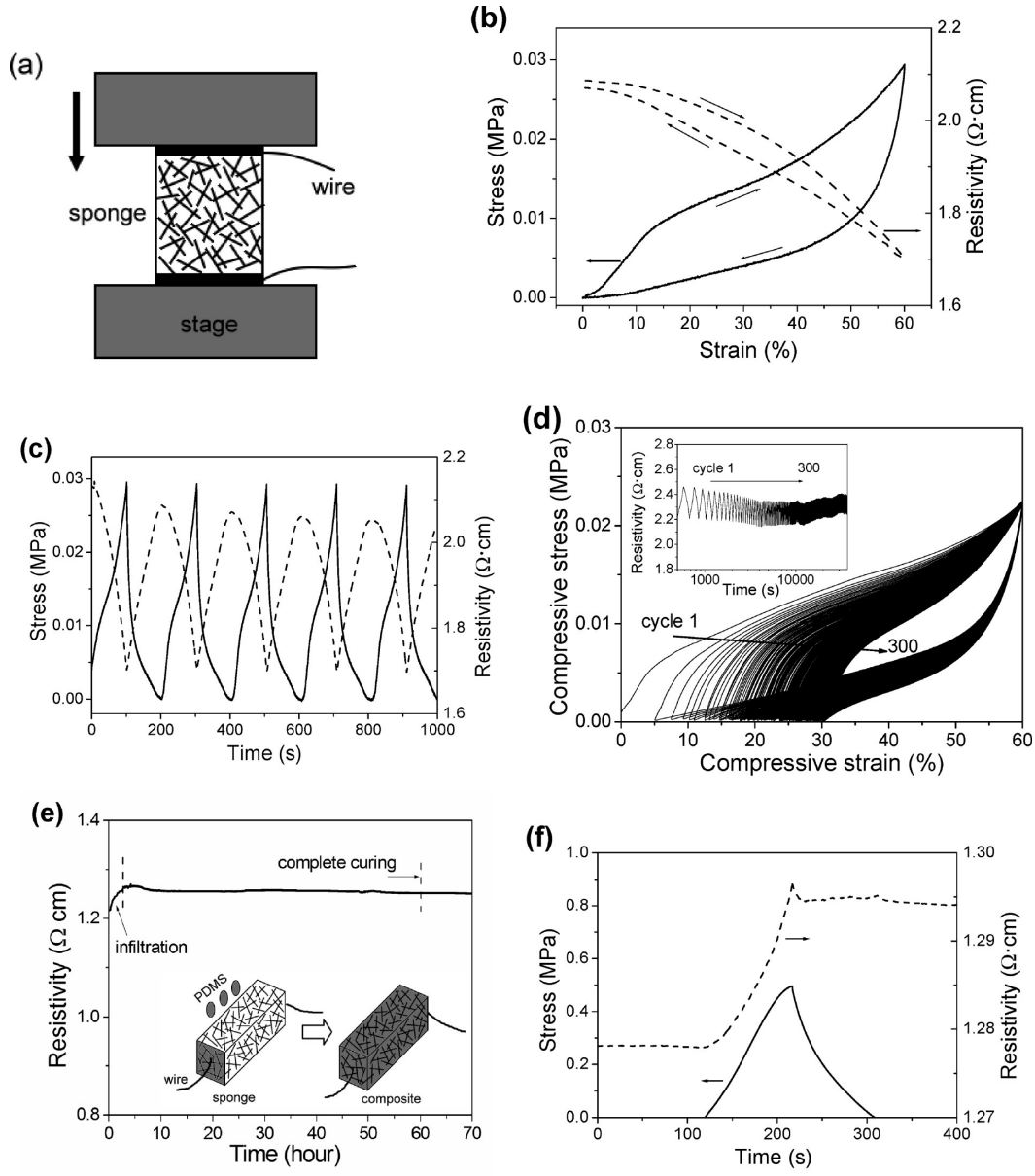

Figure 4. Sponge-based strain sensors and conductive composites. (a) Illustration of *in situ* measurement of electrical resistivity during compression. Two electrode wires are connected to the silver paste patch on top and bottom of the sponges, respectively. (b) Testing of a sponge with density of 7.3 mg/cm^3 by a preloading cycle to remove the permanent deformation. The plots show the change of compressive stress and resistivity during a compression cycle ($\varepsilon = 60\%$). (c) Reversible change of resistivity (dash) over five stress (solid) cycles. (d) Stress−strain curves of 300 cycles in a fatigue testing. Inset, sponge resistivity recorded during this period. (e) Resistivity recorded during the entire PDMS infiltration and curing process over a period of 70 h. Inset, illustration of the infiltration method in which PDMS droplets were delivered to sponges forming a composite structure after curing. (f) Irreversible change of resistivity when the sponge−PDMS composite was compressed for one cycle (occurring at time of 120−310 s).

ter 300 cycles, with a plastic deformation up to 30% (Figure 4d). With reinforcement to reduce deformation and improve fatigue behavior, the sponge sensors have the potential to work in large-strain (up to 60%) conditions for a large number of cycles (>1000).

We directly infiltrated polydimethylsiloxane (PDMS) into CNT sponges to make nanocomposites. The process involved the addition of PDMS droplets and subsequent infiltration into pores by capillarity (inset of Figure 4e). Complete curing of the composite took about 60 h. The sponge resistivity increased by 10% during the infiltration process, but then remained constant at 1.25 $\Omega \cdot$ cm during the entire curing process (Figure 4e). The results make us speculate that the percolated three-dimensional CNT network is still maintained, and the cross-linking of PDMS molecules does not disturb the contact among CNTs. Previous work has mainly focused on polymer filling of aligned CNT arrays, in which the conductivity in perpendicular to alignment drops significantly.[16−18] In addition, polyvinyl alcohol (PVA) infiltration of CNT aero-

gels consisting of loosely packed nanotubes has decreased the conductivity by 5 orders of magnitude.[19] The sponge-PDMS composites also can be compressed reversibly within a strain of 10%. However, their resistivity maintains at a higher level even after unloading, which is different from pure CNT sponges (Figure 4f). It is possible that the contact between CNTs cannot be fully recovered once it is disrupted, due to the presence of PDMS. Currently we are not clear about why the resistivity does not recover after load removal. It was observed previously that both tensile and compressive strains could disturb the CNT connectivity in the PDMS matrix.[17] In comparison, nanocomposites processed by conventional methods such as dispersing and mixing CNTs with polymers generally reach very limited conductivity even at percolation.[24] Our sponges may provide a way for fabrication of highly conductive composites at minimum CNT addition (0.94 wt %).

In summary, we developed soft, porous nanotube sponges with controlled densities ranging from 5.8 to 25.5 mg/cm^3. The lower-density sponges show high compressibility of up to 90% volume reduction, while the higher-density sponges can recover to 93% of original volume after compression. The electrical resistivity changes linearly and reversibly during large-strain compression cycles. If plastic deformation can be further reduced, the sponges have the potential to work as stress sensors. We made conductive sponge-based polymer composites with resistivity comparable to pure CNT scaffolds.

METHODS AND MATERIALS

Synthesis of CNT Sponges with Controlled Density. Ferrocene and 1,2-dichlorobenzene were used as the catalyst precursor and carbon source for CVD production of sponge-like structures. A solution of ferrocene powders dissolved in dichlorobenzene (0.06 g/mL) was injected into the CVD furnace by a syringe pump at a constant feeding rate in the range of 0.1−0.25 mL/min. The reaction temperature was 860 °C, and generally the deposition time is 4 h when the sponge reaches a thickness of about 8 mm. Carrier gas, consisting of a mixture of Ar and H_2, was flowing at a rate of 2000 and 300 mL/min, respectively. At a source feeding rate of 0.1 mL/min, the as-grown CNT sponge showed a density of 5.8 mg/cm^3. The growth rate and sponge density increases with higher feeding rate, and the density reaches 25.5 mg/cm^3 at a feeding rate of 0.25 mL/min. The sponges were typically grown on cleaned smooth quartz substrates. The sponge porosity is calculated as $(1 - \rho_{sponge}/\rho_{CNT}) \times 100$, in which ρ_{sponge} is the bulk density and ρ_{CNTs} is the CNT density. The bulk density is calculated as the mass of the sponge divided by its volume. For each data point, more than three different size samples were measured and averaged. The density of CNTs (2.3−2.4 g/cm^3) was measured by a Micromeritics Accupyc 1330 densimeter.

Characterization of Sponge Density, Porosity, And Mechanical Property. The microstructure and morphology of sponges and sponge-polymer composites were characterized by SEM (Leo 1530) and transmission electron microscope (TEM) (JEOL 2011). Mechanical tests were done by a single-column system (Instron 5843) equipped with two flat-surface compression stages and 10 N/1kN load cells. CNT sponges were cut into cubic (about 1 × 1 × 1 cm^3) or rectangular blocks. For electromechanical tests, their top and bottom sponge surfaces were coated by a uniform layer of silver paste, and a soft, thin silver wire was connected to each surface, respectively. Care was taken to ensure no penetration of silver paste into the sponge network. During compressive tests, electrical resistance (Keithley 2400, under a bias of 0.1 V) was recorded simultaneously with stress−strain curves. The top stage was set to move downward at a constant rate of 2 mm/min. Reproducible resistance data over many cycles indicate that the contact resistance (between compression stage and sponge surface) is stable and its fluctuation due to stage movement is negligible.

Composite Fabrication and Electromechanical Testing. The sponge-PDMS composite was made by direct infiltration. Droplets of PDMS (a mixture of resin and hardener at a volume ratio of 10:1) were delivered to the sponge surface one by one, and each droplet was sucked into the sponge pores within several to tens of minutes. The infiltration became slower as more PDMS droplets were delivered until saturation. Two electrodes (silver wires) were connected to the side surfaces of the sponge, and electrical resistance was monitored during the entire infiltration and subsequent curing process. It took about 60 h for the composite to completely cure at room temperature. Mechanical and electrical testing of the composite follows the same method for pure sponges.

Acknowledgment. This work is supported by Tsinghua University Initiative Scientific Research Program (Grant 2009THZ02123). A. Cao thanks the start-up support from the College of Engineering, Peking University.

REFERENCES AND NOTES

1. Hirata, E.; Uo, M.; Takita, H.; Akasaka, T.; Watari, F.; Yokoyama, A. Development of a 3D collagen scaffold coated with multiwalled carbon nanotubes. *J. Biomed. Mater., Res. B* **2009**, *90B*, 629–634.
2. Lee, C. K.; Shin, S. R.; Mun, J. Y.; Han, S.-S.; So, I.; Jeon, J.-H.; Kang, T. M.; Kim, S. I.; Whitten, P. G.; Wallace, G. G.; Spinks, G. M.; Kim, S. J. Tough supersoft sponge fibers with tunable stiffness from a DNA self-assembly technique. *Angew. Chem., Int. Ed.* **2009**, *48*, 5116–5120.
3. Svagan, A. J.; Azizi Samir, M. A. S.; Berglund, L. A. Biomimetic foams of high mechanical performance based on nanostructured cell walls reinforced by native cellulose nanofibrils. *Adv. Mater.* **2008**, *20*, 1263–1269.
4. Koerner, H.; Price, G.; Pearce, N. A.; Alexander, M.; Vaia, R. A. Remotely actuated polymer nanocomposites—Stress-recovery of carbon-nanotube-filled thermoplastic elastomers. *Nat. Mater.* **2004**, *3*, 115–120.
5. Sekitani, T.; Noguchi, Y.; Hata, K.; Fukushima, T.; Aida, T.; Someya, T. A rubberlike stretchable active matrix using elastic conductors. *Science* **2008**, *321*, 1468–1472.
6. Capadona, J. R.; Shanmuganathan, K.; Tyler, D. J.; Rowan, S. J.; Weder, C. Stimuli-responsive polymer nanocomposites inspired by the sea cucumber dermis. *Science* **2008**, *319*, 1370–1374.
7. Aliev, A. E.; Oh, J.; Kozlov, M. E.; Kuznetsov, A. A.; Fang, S.; Fonseca, A. F.; Ovalle, R.; Lima, M. D.; Haque, M. H.; Gartstein, Y. N.; *et al.* Giant-stroke, superelastic carbon nanotube aerogel muscles. *Science* **2009**, *323*, 1575–1578.
8. Anderson, M. L.; Stroud, R. M.; Rolison, D. R. Enhancing the activity of fuel-cell reactions by designing three-dimensional nanostructured architectures: Catalyst-modified carbon−silica composite aerogels. *Nano Lett.* **2002**, *2*, 235–240.
9. Moura, F. C. C.; Lago, R. M. Catalytic growth of carbon nanotubes and nanofibers on vermiculite to produce floatable hydrophobic "nanosponges" for oil spill remediation. *Appl. Catal., B* **2009**, *90*, 436–440.

10. Gui, X.; Wei, J.; Wang, K.; Cao, A.; Zhu, H.; Jia, Y.; Shu, Q.; Wu, D. Carbon nanotube sponges. *Adv. Mater.* **2010**, *22*, 617–621.
11. Leventis, N.; Sotiriou-Leventis, C.; Zhang, G.; Rawashdeh, A.-M. M. Nanoengineering strong silica aerogels. *Nano Lett.* **2002**, *2*, 957–960.
12. Capadona, L. A.; Meador, M. A. B.; Alunni, A.; Fabrizio, E. F.; Vassilaras, P.; Leventis, N. Flexible, low-density polymer crosslinked silica aerogels. *Polymer* **2006**, *47*, 5754–5761.
13. Futaba, D. N.; Hata, K.; Yamada, T.; Hiraoka, T.; Hayamizu, Y.; Kakudate, Y.; Tanaike, O.; Hatori, H.; Yumura, M.; Iijima, S. Shape-engineerable and highly densely packed single-walled carbon nanotubes and their application as super-capacitor electrodes. *Nat. Mater.* **2006**, *5*, 987–994.
14. Chang, W. T.; Noh, S. S.; Tabib-Azar, M. High-efficiency and flow-ratio-dependent growth of carbon nanotubes and carbon spheres hybrid. *Phys. B* **2009**, *404*, 1154–1158.
15. García-Martínez, J.; Lancaster, T. M.; Ying, J. Y. Synthesis and catalytic applications of self-assembled carbon nanofoams. *Adv. Mater.* **2008**, *20*, 288–292.
16. Huang, H.; Liu, C.; Wu, Y.; Fan, S. Aligned carbon nanotube composite films for thermal management. *Adv. Mater.* **2005**, *17*, 1652–1656.
17. Jung, Y. J.; Kar, S.; Talapatra, S.; Soldano, C.; Viswanathan, G.; Li, X.; Yao, Z.; Ou, F. S.; Avadhanula, A.; Vajtai, R.; *et al*. Aligned carbon nanotube-polymer hybrid architectures for diverse flexible electronic applications. *Nano Lett.* **2006**, *6*, 413–418.
18. Yaglioglu, O.; Martens, R.; Hart, A. J.; Slocum, A. H. Conductive carbon nanotube composite microprobes. *Adv. Mater.* **2008**, *20*, 357–362.
19. Bryning, M. B.; Milkie, D. E.; Islam, M. F.; Hough, L. A.; Kikkawa, J. M.; Yodh, A. G. Carbon nanotube aerogels. *Adv. Mater.* **2007**, *19*, 661–664.
20. Cao, A.; Dickrell, P. L.; Sawyer, W. G.; Ghasemi-Nejhad, M. N.; Ajayan, P. M. Super-compressible foamlike carbon nanotube films. *Science.* **2005**, *310*, 1307–1310.
21. Deck, C. P.; Flowers, J.; McKee, G. S. B.; Vecchio, K. Mechanical behavior of ultralong multiwalled carbon nanotube mats. *J. Appl. Phys.* **2007**, *101*, 023512.
22. Liu, P.; Liu, L.; Wei, Y.; Sheng, L.; Fan, S. Enhanced field emission from imprinted carbon nanotube arrays. *Appl. Phys. Lett.* **2006**, *89*, 073101-1–073101-3.
23. Suhr, J.; Victor, P.; Ci, L.; Sreekala, S.; Zhang, X.; Nalamasu, O.; Ajayan, P. M. Fatigue resistance of aligned carbon nanotube arrays under cyclic compression. *Nat. Nanotechnol.* **2007**, *2*, 417–421.
24. Grossiord, N.; Loos, J.; Regev, O.; Koning, C. E. Toolbox for dispersing carbon nanotubes into polymers to get conductive nanocomposites. *Chem. Mater.* **2006**, *18*, 1089–1099.